Supplemental Materials — Chutkow et. al., "Deletion of the α-arrestin protein Txnip in mice promotes adipogenesis and adiposity while preserving insulin sensitivity."

SUPPLEMENTAL METHODS

Basal Study. Fat and lean body masses were assessed by ^{1}H magnetic resonance spectroscopy (Bruker BioSpin, Billerica, MA) before and after 4 weeks of high-fat diet. Comprehensive animal metabolic monitoring system (CLAMS; Columbus Instruments, Columbus, OH) was used to evaluate activity, food consumption, and energy expenditure (EE). EE and food intake were normalized to total body weight. EE and RQ were calculated from the gas exchange data [energy expenditure = $(3.815 + 1.232 \times RQ) \times VO_2$], with RQ determined as the ratio of VCO_2 to VO_2. Activity was measured in both horizontal and vertical directions using infrared beams to count the beam breaks during a specified period. Feeding was measured by recording the difference in the scale measurement of the center feeder from one time point to another.
Analysis of EE was subjected to three methods of body mass indexing. 1) Body-mass normalized: Hourly EE values for each mouse were normalized to their total body mass (or lean mass derived from MRS analysis). Mice were monitored for 72h and total EE was calculated as the area under the curve over the monitoring period, averaged to a 24h period; 2) Whole-mouse normalized: The same measured hourly EE values for each mouse monitored over 72h were average to a 24h period without normalizing to each individual mouse's body mass; 3) Analysis of Covariance (ANCOVA): The same unindexed hourly EE values for each mouse monitored over 72h were average to a 24h period, then subjected to an analysis of covariance (ANCOVA) between mouse strains with each individual's body weight serving as the covariant to its EE in the ANCOVA calculation. 24h averaged EE for each mouse within a group was initially plotted as a function of its mass and linear regression was performed by the method of least squares and goodness of fit was confirmed by analysis of the plot of residuals. One-way ANCOVA was then used to compare the groups using a web-based calculator provided by Vassar College: (http://faculty.vassar.edu/lowry/VassaStats.htm). ANCOVA was also performed using 'lean body mass' rather than total body mass, as determined by MRS.

Hyperinsulinemic-euglycemic clamp studies. HE clamp studies were conducted as described previously (1). Briefly, mice were surgically cannulated with a catheter into the right jugular vein 7 days before study, and then subjected to a standardized clamp protocol. Overnight fasted mice were continuously infused with 0.05μCi/min 3-^{3}H-glucose over 2h to assess basal glucose turnover. Subsequently, hyperinsulinemic-euglycemic clamping was conducted for 140 minutes with a primed/continuous infusion of human insulin (21 mU/kg prime over 3 minutes, 3 mU/kg per minute infusion; Novo Nordisk) and a variable infusion of 20% dextrose to maintain euglycemia (120 mg/dl). 0.1μCi/min 3-^{3}H-glucose were continuously infused during the clamp period to determine insulin stimulated glucose uptake and endogenous glucose production after the basal period. A 10μCi bolus of 2-deoxy- d-[1-^{14}C]glucose (PerkinElmer) was injected 85 minutes into the clamp to estimate the rate of insulin-stimulated tissue glucose uptake. Additional blood samples (20–60 μl) were taken at 0 and 135 minutes to determine plasma fatty acid and insulin concentrations. At study completion mice were anesthetized and tissues were taken within 3 minutes, flash frozen with liquid N_2–cooled aluminum tongs, and stored at –80°C for subsequent analysis.

Calculations for basal and insulin-stimulated whole body glucose turnover. Basal and insulin-stimulated whole body glucose turnover rates were determined as the ratio of the [3-^{3}H]glucose infusion rate (in dpm) to the specific activity of plasma glucose (dpm per mg) at the end of the basal period and during the final 30 min of the clamp experiment, respectively. Hepatic glucose production was determined by subtracting the glucose infusion rate from the rate of total glucose appearance. The plasma concentration of ^3H_2O was determined by the difference between ^{3}H counts without and with drying; whole body glycolysis was calculated from the rate of increase in plasma ^3H_2O concentration, determined by linear regression of the measurements at 90, 100, 110, 120, 130, and 140 min. Whole body glycogen synthesis was estimated by subtracting whole body glycolysis from whole body glucose uptake. Tissue ^{14}C-2-deoxyglucose-6-phosphate content was measured following sample homogenizing, and the supernatant's ^{14}C-2-deoxyglucose-6-phosphate was separated from 2-deoxyglucose by ion-exchange column as previously described (2).

Adipose tissue biopsy and cell size analysis. Adipocyte sizing using a Beckman Coulter Multisizer III was performed as previously described (3). 20–30 mg of excised epididymal fat tissue was immediately placed in osmium tetroxide for 48h fixation at 37°C. Cell size was determined by a Beckman Coulter Multisizer III with a 400µm aperture, set to count 6,000 particles. Data were expressed as particle diameters and displayed as histograms of counts against diameter. Adipose cell size distribution, nadir (defined as the frequency low point between the two cell populations), and the proportion of cells above and below the nadir point were calculated by the Multisizer software and expressed as '% above' (% large cells) and '% below' (% small cells) the nadir. In addition, the 'peak diameter' of the large adipose cells was defined as the mean diameter at which the frequency of the large cell population reached a maximum. The Multisizer software also calculated the mean, median and mode of the overall cell size for each sample.

Endogenous PPAR and exogenous PPARg-LBD reporter assays. Generation and transduction of Txnip lentiviral species is described previously (4). Txnip shRNA and control shRNA plasmids were purchased from Sigma and pseudoviral particles were generated as described (4). 3T3-L1 pre-adipocytes (ATCC) were generated to stably overexpress Txnip, empty vector control, scrambled negative control shRNA, or Txnip shRNA species by puromycin selection following viral transduction. Txnip expression levels were confirmed by Western blot analysis with anti-Txnip antibodies as previously described (5). For reporter activity assays 3T3-L1 stable cell lines were seeded in 24-well plates at 1 x 10^5 cells per well and transfected the following day with plasmids described below using Transit-LT1 (Mirus Bio) per the manufacturer's instructions. For PPRE activity, cells were transfected with 600ng of pDR-1 $PPRE_3$-TK-Luc reporter plasmid (6) + 150ng sv40-βgal plasmid for normalization. For PPARγ ligand-binding (LBD) activity, cells were transfected with 300ng/well MH-TK-LUC luciferase reporter, 300ng/well Gal4-PPARg-LBD (6) and 125ng/well CMV-bgal for transfection normalization. The following day cells were incubated in media with 1% delipidated FCS (Sigma) for 12 hrs, then treated with varying rosiglitazone concentrations or DMSO control for 18 hours. Cells were lysed in Passive Lysis Buffer (Promega), and lysates were assayed for luciferase or β˜galactosidase activity with Luciferase Assay (Promega) and Galacto-Light Plus Assay. Luciferase activity was normalized to β̃galactosidase activity.

Glyceroneogenesis measurement in 3T3-L1 adipocytes. *De novo* glycerol formation was assessed by ^{14}C pyruvate incorporation in cultured 3T3-L1 adipocytes essentially as described (7). 3T3-L1 adipocytes were differentiated and transduced with Txnip overexpressing lentivirus, Txnip shRNA lentivirus, or relevant control lentivirus at d8 post differentiation as previously described (8). 96h post transduction, adipocytes were serum-withdrawn in DMEM supplemented with 0.3% FFA-free BSA for 3h. Adipocytes were incubated in the presence of ^{14}C pyruvate in KHB Buffer/0.3% FA-free BSA at 37°C for 2h under 5% CO_2. The adipocytes were rinsed with PBS and scraped into 10mM Tris-Cl pH 7.4, containing 0.25M sucrose, 0.1mM EDTA, 0.1mM DTT, 0.1% Triton, and frozen in liquid nitrogen vapor before lipid extraction. Lipids were collected by chloroform extraction according to the method of Bligh and Dyer (9), and ^{14}C pyruvate incorporation was assessed by liquid scintillation counting of the chloroform fraction and normalized to cellular protein levels.

Adipose Histology and Immunofluorescence. Epididymal white adipose tissue was immediately excised from euthanized mice, wash in ice cold PBS, and then fixed over night in PLP Fixative at 4°C (10), and stored in 70% ethanol at 4°C until paraffin embedding. Sections were either H & E stained, or stained with anti-CD68 antibodies (rabbit polyclonal, Santa Cruz). Immunofluorescence was performed using Alexa 488 anti-rabbit secondary antibodies (Invitrogen) and nuclei were DAPI counterstained.

mRNA quantification by real-time PCR. Epididymal white adipose tissue total RNA was isolated using Trizol reagent per manufacturer's instructions (Invitrogen). cDNA was synthesized from 1µg of total RNA and random hexamers using the TaqMan Reverse Transcription kit (Applied Biosystems) and real time PCR was performed in a 7300 Real-time PCR system (Applied Biosystems), with 40 cycles of: 95°C x 15 sec., 60°C x 1 min. All reactions were performed in triplicate and verified by melting curve analysis. Relative amount of mRNA was normalized to TATA-binding protein (TBP) transcript levels. All reactions except TBP were SYBR green based with primers at a final [ ] = 500nM each. 1µl diluted cDNA was used per 20µl reaction from an initial input of 1µg total RNA diluted to a final volume of 800µl following cDNA reverse transcription

TATA Box Binding protein real-time PCR was performed as a Taqman assay using commercially defined primer + probe (ABI, Mm00446973_m1) and 1µl of diluted cDNA. TBP expression was validated to 18S for each genotype and dietary condition, both to validate the linear expression range and verify invariant expression levels relative to diet and genotype. All transcript expression levels were normalized to TBP expression.

Primer sequences are:

Gene Symbol	Gene Bank	Forward / Reverse
ACCα	NM_133366	F 5’ – ATGGGCGGAATGGTCTCTTTC
		R 5’ – TGGGGACCTTGTCTTCATCAT
Adiponectin	NM_009605	F 5' – GCAGGCATCCCAGGACATC
		R 5' – GCGATACATATAAGCGGCTTCT
Fabp4 (AP2)	NM_024406	F 5' – AGAAGTGGGATGGAAAGTCG
		R 5' – TGGCTCATGCCCTTTCATA
Scarb2 (CD36)	NM_007644	F 5' – AGAAGGCGGTAGACCAGAC
		R 5' – GTAGGGGGATTTCTCCTTGGA
FAS	NM_007988	F 5’ – GGAGGTGGTGATAGCCGGTAT
		R 5’ – TGGGTAATCCATAGAGCCCAG
GLUT1	NM_011400	F 5' – CAGTTCGGCTATAACACTGGTG
		R 5' – GCCCCCGACAGAGAAGATG
GLUT4	NM_009204	F 5' – GTGACTGGAACACTGGTCCTA
		R 5' – CCAGCCACGTTGCATTGTAG
Leptin	NM_008493	F 5' – GAGACCCCTGTGTCGGTTC
		R 5' – CTGCGTGTGTGAAATGTCATTG
LPL	NM_008509	F 5' – GGGAGTTTGGCTCCAGAGTTT
		R 5' – TGTGTCTTCAGGGGTCCTTAG
PC	NM_008792	F 5' – GGGACTCCTTTGGACACAGA
		R 5' – GCCCCTTCCCAGTACTCACT
PEPCK	NM_011044	F 5’ – ACTCGGATGGGCATATCTGT
		R 5’ – GCCCAGTTGTTGACCAAAG
Pgc1a (PGC1α)	NM_008904	F 5' – GAAAGGGCCAAACAGAGAGA
		R 5' – GAAAGGGCCAAACAGAGAGA
Ppparg2 (PPARγ2)	NM_011146	F 5' – ACTGCCTATGAGCACTTCAC
		R 5' – CAATCGGATGGTTCTTCGGA
Rn18S	NR_003278	F 5' – CCATCCAATCGGTAGTAGCG
		R 5' – GTAACCCGTTGAACCCCATT
Txnip	NM_023719	F 5' – ATCCCAGATACCCCAGAAGC
		R 5' – TGAGAGTCGTCCACATCGTC
UCP2	NM_011671	F 5' – ATGGTTGGTTTCAAGGCCACA
		R 5' – CGGTATCCAGAGGGAAAGTGAT
Tbp	NM_013684.3	**

SUPPLEMENTAL FIGURE LEGENDS.

Supplemental Figure 1 — SCD and HFD weights (A) Weights for WT and Txnip KO mice pre and post HFD as assessed by ^{1}H magnetic resonance spectroscopy**.** * $p<0.05$. (B) Mass of individual fat depots for WT and Txnip KO mice obtained after 4 weeks of SCD-feeding or HFD-feeding. SC = subcutaneous fat harvested from the gluteal depot; Epidid = epididymal visceral fat depot; Brown = scapular brown fat depot. * $p<0.05$.

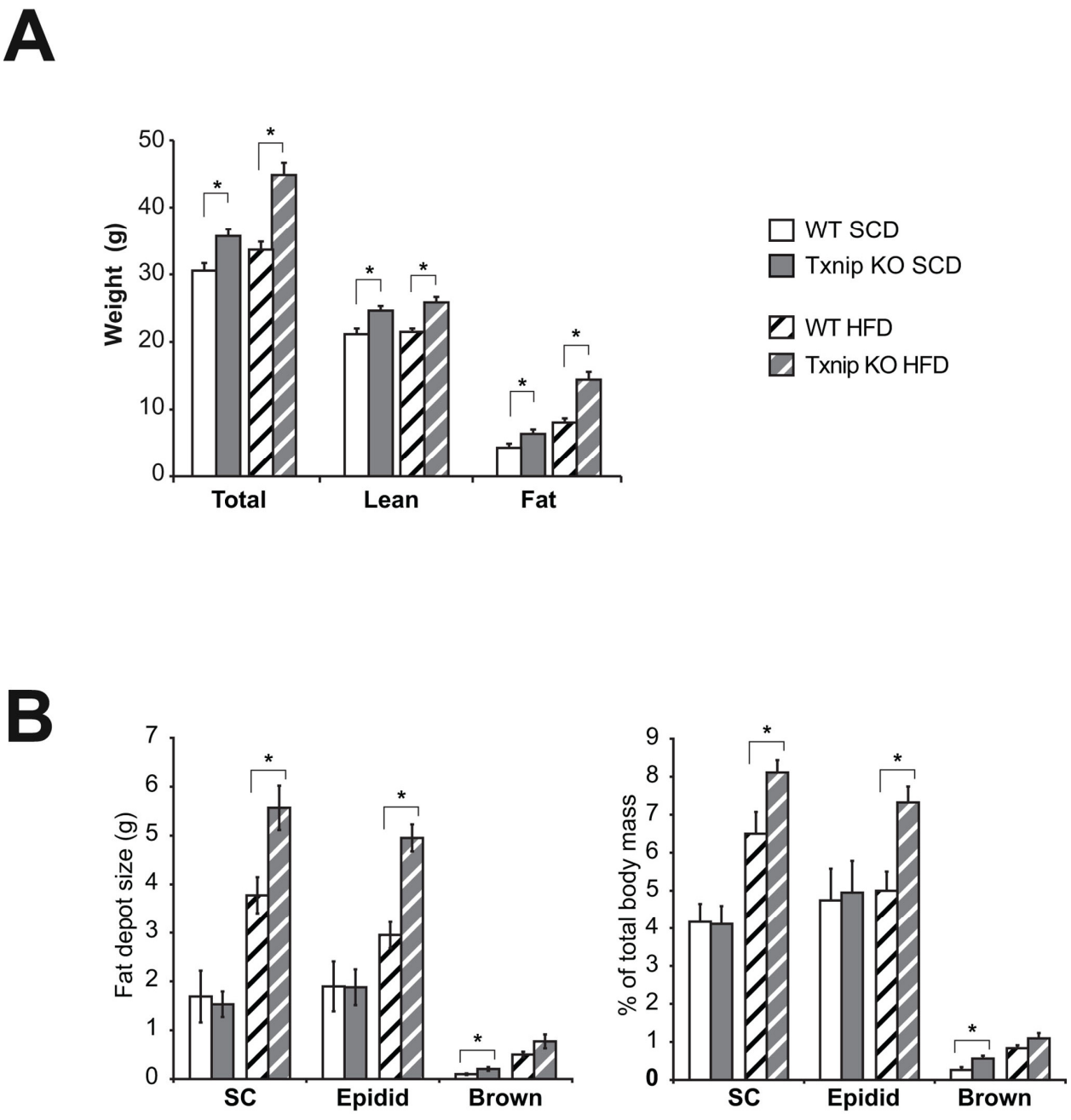

Supplemental Figure 2 — Basal vs clamped hepatic glucose production following HFD. Basal and post-clamp hepatic glucose production for WT and Txnip KO mice after 4 weeks HFD, as determined by labeled glucose precursor infusion during in vivo euglycemic-hyperinsulinemic clamp studies. Glucose production was determined by ^{3}H-glucose infusion throughout the euglycemic-hyperinsulinemic clamp protocol.

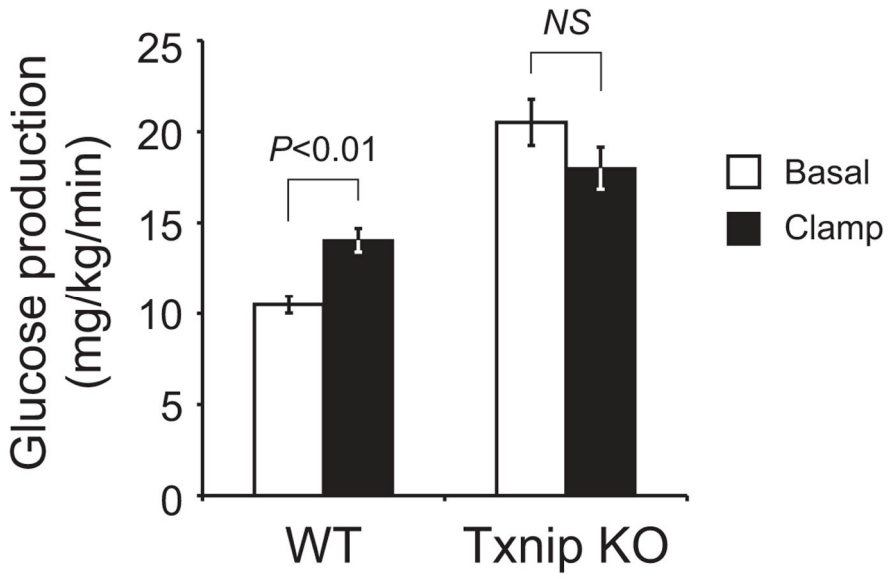

Supplemental Figure 3 — CD68+ infiltrate into visceral adipose tissue and measurement of serum inflammatory markers. (A) Examples of visceral white adipose tissue with immunofluorescent CD68+ staining in both WT and Txnip KO mice following 4 weeks HFD, with 'IgG control' from a WT mouse (below) illustrating the negative control. (B) TNFα and IL-6 serum levels for WT and Txnip KO mice following 4 weeks HFD feeding. *n*=7 for each group.

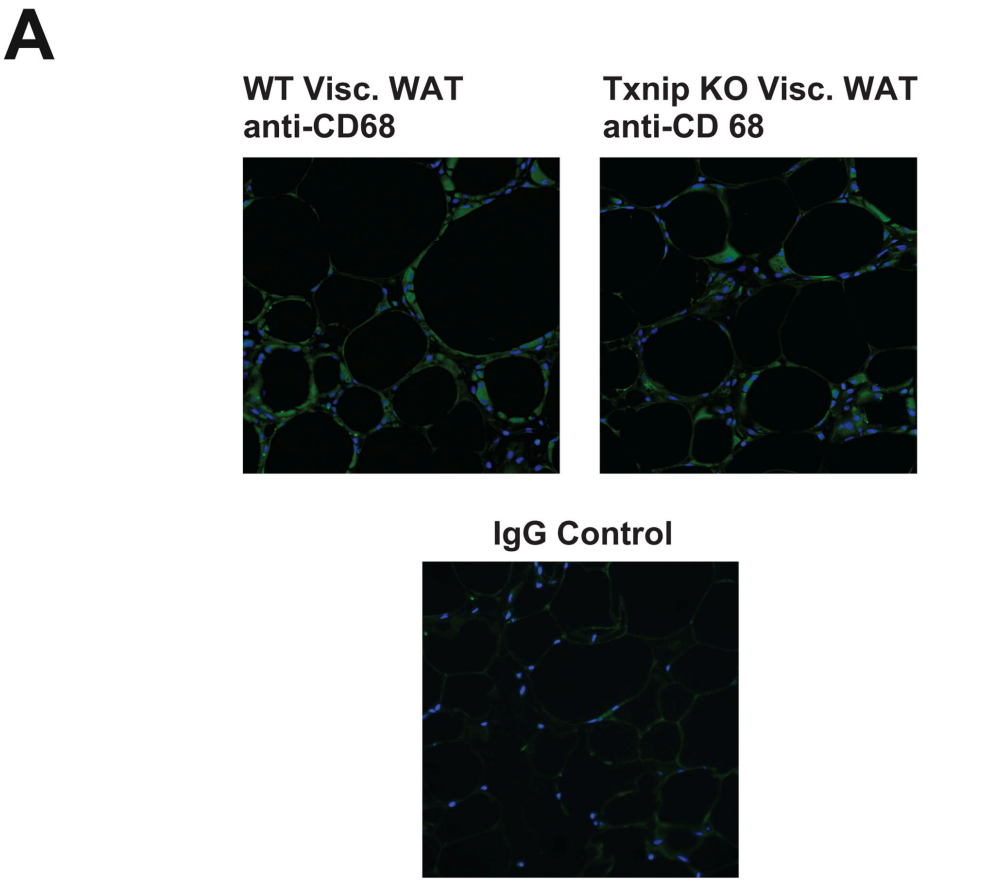

Supplemental Figure 4 — Txnip mRNA temporal expression during 3T3-L1 adipocyte differentiation, and expression in adipose tissue following HFD. (A) Txnip mRNA expression was determined by real-time PCR at various time points during 3T3-L1 adipocyte differentiation. 'd0' 3T3-L1 are 2d post-confluent. Differentiation was induced with standard DMI application, indicated by arrow. 1μM rosiglitazone or DMSO vehicle control were applied during the final 12 hours of each timepoint. Values are relative to Txnip expression in undifferentiated 3T3-L1, and are normalized to TBP expression. *n*=5 replicates per group. (B) Real-time PCR quantification of Txnip mRNA expression from epididymal WAT in WT mice after 4 weeks of HFD, compared to age-matched WT mice fed a SCD over the same period. *n*=8 mice per group.

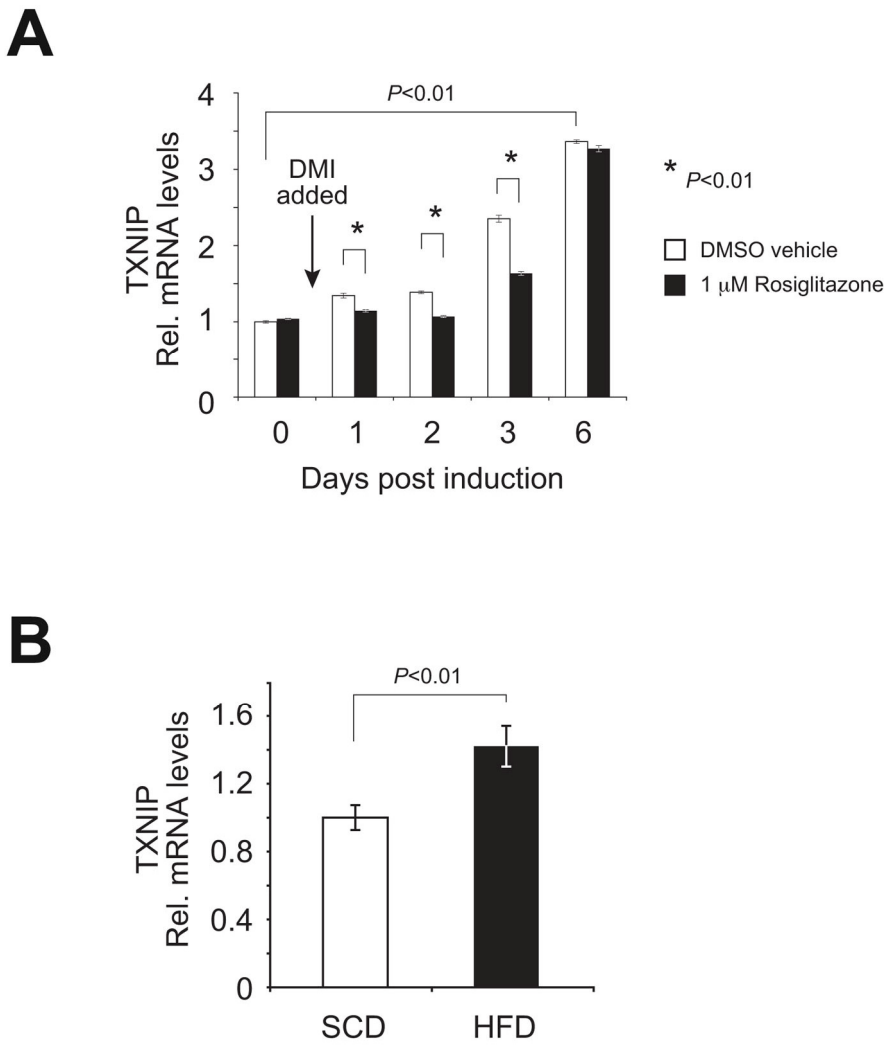

SUPPLEMENTAL REFERENCES.

1. Samuel VT, Liu ZX, Wang A, Beddow SA, Geisler JG, Kahn M, Zhang XM, Monia BP, Bhanot S, Shulman GI: Inhibition of protein kinase Cepsilon prevents hepatic insulin resistance in nonalcoholic fatty liver disease. *J Clin Invest* 117:739-745, 2007

2. Youn JH, Buchanan TA: Fasting does not impair insulin-stimulated glucose uptake but alters intracellular glucose metabolism in conscious rats. *Diabetes* 42:757-763, 1993

3. McLaughlin T, Sherman A, Tsao P, Gonzalez O, Yee G, Lamendola C, Reaven GM, Cushman SW: Enhanced proportion of small adipose cells in insulin-resistant vs insulin-sensitive obese individuals implicates impaired adipogenesis. *Diabetologia* 50:1707-1715, 2007

4. Chutkow WA, Patwari P, Yoshioka J, Lee RT: Thioredoxin-interacting protein (Txnip) is a critical regulator of hepatic glucose production. *J Biol Chem* 283:2397-2406, 2008

5. Yoshioka J, Imahashi K, Gabel SA, Chutkow WA, Burds AA, Gannon J, Schulze PC, MacGillivray C, London RE, Murphy E, Lee RT: Targeted deletion of thioredoxin-interacting protein regulates cardiac dysfunction in response to pressure overload. *Circ Res* 101:1328-1338, 2007

6. Nagy L, Tontonoz P, Alvarez JG, Chen H, Evans RM: Oxidized LDL regulates macrophage gene expression through ligand activation of PPARgamma. *Cell* 93:229-240, 1998

7. Cadoudal T, Distel E, Durant S, Fouque F, Blouin JM, Collinet M, Bortoli S, Forest C, Benelli C: Pyruvate dehydrogenase kinase 4: regulation by thiazolidinediones and implication in glyceroneogenesis in adipose tissue. *Diabetes* 57:2272-2279, 2008

8. Patwari P, Higgins LJ, Chutkow WA, Yoshioka J, Lee RT: The interaction of thioredoxin with Txnip. Evidence for formation of a mixed disulfide by disulfide exchange. *J Biol Chem* 281:21884-21891, 2006

9. Bligh EG, Dyer WJ: A rapid method of total lipid extraction and purification. *Can J Biochem Physiol* 37:911-917, 1959

10. McLean IW, Nakane PK: Periodate-lysine-paraformaldehyde fixative. A new fixation for immunoelectron microscopy. *J Histochem Cytochem* 22:1077-1083, 1974